Synthesis of CO2-philic Xanthate-Oligo(vinyl acetate)Based Hydrocarbon Surfactants by RAFT Polymerization and Their Applications on Preparation of Emulsion-Templated Materials

ARTICLE *in* MACROMOLECULES · NOVEMBER 2010

Impact Factor: 5.8 · DOI: 10.1021/ma101182f

Macromolecules
ARTICLE

Macromolecules **XXXX**, *XXX*, 000–000 **A**
DOI: 10.1021/ma101182f

Synthesis of CO_2-philic Xanthate−Oligo(vinyl acetate)-Based Hydrocarbon Surfactants by RAFT Polymerization and Their Applications on Preparation of Emulsion-Templated Materials

Keping Chen,[†] Neil Grant,[‡] Liyun Liang,[†] Haifei Zhang,[‡] and Bien Tan*[,†]

[†]*School of Chemistry and Chemical Engineering, Huazhong University of Science and Technology, Wuhan 430074, China, and* [‡]*Department of Chemistry, University of Liverpool, L69 7ZD, Liverpool, U.K.*

Received May 28, 2010; Revised Manuscript Received October 1, 2010

ABSTRACT: Amphiphilic block copolymers poly(ethylene glycol)-*block*-oligo(vinyl acetate) (PEG-*b*-OVAc) and OVAc-*b*-PEG-*b*-OVAc have been demonstrated to be effective surfactants for CO_2-in-water (C/W) emulsions. However, the high cost and difficulty of synthesis process can render the economics of CO_2 process unfavorable. In this work, by reversible addition−fragmentation chain transfer (RAFT) polymerization, a series of well-defined CO_2-philic triblock copolymers X−OVAc-*b*-PEG-*b*-OVAc−X (where X stands for xanthate group) were synthesized. The structures and molecular weights of these copolymers were characterized by ^{1}H NMR and GPC. The results of GPC analysis exhibited relatively narrow polydispersity (PDI < 1.35). The process of preparation of X−OVAc-based surfactants was much more simple, inexpensive and also easy to control, which could promote industrial-scale applications. The X−OVAc-based surfactants were found effectively to produce highly concentrated stable C/W emulsions. Porous emulsion-templated materials were prepared by the polymerization of the continuous phase of C/W emulsions. The open-cell morphology of the emulsion-templated materials was evidenced by scanning electron microscope. To tune the morphology of the porous structures, the influence of the surfactant concentration and molecular weight of OVAc block were also investigated. It was shown that X−OVAc-based surfactants can outperform perfluorinated surfactants and approach OVAc-based surfactants for such applications.

Introduction

Emulsion templating is a relatively versatile method for the preparation of highly porous organic[1−3] and inorganic materials,[4] which are extremely useful in a wide range of applications including catalysis,[5] chromatography,[6] and drug delivery,[7] etc. In general, high internal phase emulsion (HIPE) with the droplet phase volume fraction occupying more than 74.05% v/v of the emulsion volume, is initially formed, and then the continuous phase locks in the emulsion geometry usually by reaction-induced phase separation (e.g., free-radical polymerization, sol−gel chemistry). Subsequent removal of the internal phase gives rise to a porous replica of the emulsion.

In practice, a significant disadvantage is that concentrated oil-in-water (O/W) emulsion technique requires a large amount of organic solvent as internal phase, more than 75% v/v typically. Moreover it is always difficult to remove the solvent from the templated material at the end of the reaction. For inorganic materials, high temperature (> 600 °C) is required in order to completely remove any organic residues.[4] Under such circumstances, complete removal of the template phase may be much more problematic, particularly for applications such as biomaterials, where organic solvent residues are undesirable.

As a possible solution to this problem, high internal phase CO_2-in-water (C/W) emulsions have been considered. Supercritical carbon dioxide ($scCO_2$) has been extensively promoted as an environmentally benign solvent because of its intriguing characters.[8] In particular, for polymers synthesis and processing, CO_2 has been recognized as a versatile solvent.[9−12] However, CO_2 is relatively a poor solvent and the majority of materials, such as polar biomolecules, pharmaceutical actives, and high molecular weight polymers, tend to exhibit low solubility in CO_2.[13,14] So far, only fluorinated polymers[15] and silicones[16] show high solubility in CO_2, which have been exploited as CO_2-philic building blocks to produce surfactants for extraction,[17] dispersion[14,18−20] and emulsion[21,22] polymerization. However, the associated costs and low biodegradability may prohibit their industrial-scale applications. A great challenge for application of CO_2 is the discovery of inexpensive CO_2-philic materials or CO_2-philes, which can preferably be easily biodegradable.[23] Inexpensive poly(ether carbonate) (PEC) and poly(ether ester) (PEE),[24,25] sugar acetates,[26−28] which are regarded as renewable CO_2-philes, have also been reported to be high CO_2 solubility, however, associated with numerous practical difficulties. Recently, various studies have been devoted to other hydrocarbon CO_2-philes,[29−32] including the influence of end-groups on their solubility.[33,34] In our previous study, we have reported that oligo(vinyl acetate) (OVAc) also exhibited anomalously high solubility in CO_2 with respect to other vinyl hydrocarbon polymers.[35−37] The end-functional OVAc was used as CO_2-philic building block to combine with poly(ethylene glycol) (PEG) to produce amphiphilic block copolymers PEG-*b*-OVAc and OVAc-*b*-PEG-*b*-OVAc, referred to as OVAc-based surfactants. Inspired by the study of these copolymers on stabilizing high internal phase C/W emulsions, we have templated those emulsions to generate highly porous open-cell poly(acrylamide) (PAM)[38] and poly(vinyl alcohol) (PVA)[39] materials in the absence of any organic solvents, but only water and CO_2. The results indicated that OVAc-based surfactants were functionally superior to perfluorinated materials for such applications, in addition to being potentially inexpensive and biodegradable.

However, there are several key limitations associated with our previous approach.[37−39] First of all, the narrow polydispersity

*Corresponding author. E-mail: bien.tan@mail.hust.edu.cn.

OVAc is obtained through a two-step process. The first step is the synthesis of the starting poly(vinyl acetate) (PVAc) with a considerable board polydispersity (PDI > 1.6). Subsequently, the starting PVAc is required to fractionate using a supercritical fluid extraction method to provide low molecular weight fractions with narrow polydispersity (PDI = 1.14−1.40). Moreover, this procedure involves supercritical fluid extraction method, which not only increases the capital equipment costs, but also is difficult to control. Second, the yield of recovered low molecular weight fractions is as low as 0.8−4.0% w/w. Moreover, the C/W emulsions stabilized by OVAc-based surfactants encounter phase separation by the addition of monomer such as acrylamide (AM). These limitations would prohibit industrial-scale applications of these materials.

Reversible addition−fragmentation chain transfer (RAFT) radical polymerization has been used extensively for the synthesis of novel complex architecture polymers, such as block copolymers,[40] combs,[41] and stars[42,43] polymers. Generally speaking, controlled/living radical polymerizations, such as nitroxide-mediated polymerization (NMP), atom transfer radical polymerization (ATRP), could also be adopted as synthetic routes. However, these methods have several limitations. The former usually requires relatively high temperature,[44] while the latter is often limited by monomer functionality and solvent selection for proper catalyst activity.[45] In addition, vinyl acetate (VAc) propagating radical is highly reactive and apt to chain transfer and termination reactions. So far, RAFT polymerization of VAc with xanthates[46−48] and cobalt-mediated radical polymerization[49,50] of VAc have proved to be the most successful method. Recently, a well-defined PVAc-*b*-PEG diblock copolymer was synthesized by RAFT polymerization using a xanthate end-functional PEG as chain transfer agent, but they did not obtain triblock copolymer (OVAc-*b*-PEG-*b*-OVAc).[51] Tong et al. has also reported the synthesis of triblock copolymer (PVAc-*b*-PEG-*b*-PVAc) with high molecular weight ($M_{n\text{-GPC}}$ > 23500 g/mol), which was not suitable for generation of C/W emulsions due to the less CO_2-philic PVAc block.[52]

In this study, we present a solution to each of the problems outlined above and show that a series of CO_2-philic xanthate end-functional triblock copolymers X−OVAc-*b*-PEG-*b*-OVAc−X with narrow PDI, where X stands for xanthate group, are directly synthesized by RAFT polymerization. Xanthate end-functional PEG (X−PEG−X) acted as macromolecular chain transfer agent (macroCTA) to medicate the polymerization of VAc. The X−OVAc-based copolymers are found extremely effective in the production of C/W emulsions with enhanced stabilities. Porous C/W emulsion-templated PAM-based materials with significantly increased levels of porosity are prepared, even without using PVA which virtually acts as "cosurfactant". The influence of surfactant concentration and molecular weight of OVAc block on the preparation of C/W emulsion-templated PAM-based materials are investigated in more detail.

Experimental Section

Materials. Vinyl acetate (VAc, Sinopharm, 97%) was freed from inhibitor by passing through an alumina column. 2,2′-azobis-(isobutyronitrile) (AIBN, Sinopharm, 80%) was recrystallized twice from ethanol. Potassium persulfate (KPS, Sinopharm, 99%) was recrystallized twice from water. Acrylamide (AM, 98%), *N,N*′-methylene bis(acrylamide) (MBAM, 98%), tetramethyl ehylenediamine (98%), ethanol(99%), carbon disulfide (99%), pyridine (99%), potassium hydroxide (KOH, 82%), 2-bromopropionyl bromide (98%), anhydrous magnesium sulfate (99%), ammonium chloride (99%), sodium bicarbonate (99%), tetrahydrofuran (THF, 99%), dichloromethane (99%), were all purchased from Sinopharm and used as received. Poly(vinyl alcohol) (PVA, Aladdin, M_w = 74800 g/mol, 99% hydrolyzed). Poly(ethylene glycol) diol (PEG, Aldrich, M_w = 600 g/mol, M_w = 2000 g/mol, and M_w = 3400 g/mol). High purity carbon dioxide (99.99%) was purchased from Ming Hui Gas.

Synthesis of Potassium *O*-Ethyl Dithiocarbonate. In a 100 mL round-bottom flask fitted with a reflux condenser, 10.50 g (0.19 mol) of potassium hydroxide was added to 30.10 g ethanol, and the mixture was heated under reflux for 1 h. After cooling in an ice bath, carbon disulfide (14.65 g, 0.19 mol) was then slowly added to the resulting wine-red solution, resulting in almost a solid piece. The crystals were filtered off and washed with ether (3 × 10 mL). The crude product (31.12 g) was recrystallized from absolute ethanol (80 mL), and light yellow needle-shaped crystals were obtained (18.39 g, 61.3%).

Synthesis of X−EG_{45}−X. The synthesis of macroCTA X−EG_{45}−X was based on methods described previously.[51] For the synthesis of macroCTAs X−EG_{13}−X and X−EG_{77}−X, the same procedure was applied. Briefly, Poly(ethylene glycol) diol (HO−EG_{45}−OH, 19.22 g, 9.61×10^{-3} mol) was placed in a 250 mL three-neck round-bottom flask and stirred with pyridine (4.0 mL) in dichloromethane (150 mL). When the reactant dissolved, the reaction was placed in an ice bath. 2-bromopropionyl bromide (5.1 mL, 4.80×10^{-2} mol) was added dropwise for 2 h. The mixture was kept stirring for further 17 h at room temperature. A white precipitate was filtered off. Dichloromethane (200 mL) was added. The resulting solution was washed with saturated ammonium chloride (4 × 100 mL), saturated sodium bicarbonate (4 × 100 mL), water (3 × 100 mL), dried over anhydrous magnesium sulfate, and then filtered off. The solvent was evaporated under vacuum. 2-bromopropionic acid poly(ethylene glycol) ester (Br−EG_{45}−Br) was finally obtained (18.71 g, 85.8%). ^{1}H NMR data (400 MHz, $CDCl_3$): δ 4.41 (q, J = 6.8 Hz, 2H, C*H*-CH_3), δ 4.32 (m, 4H, $CH_2OC(O)$), δ 3.65 (s), δ 3.5−3.8 (m, 183H, CH_2CH_2O of PEG backbone), δ 1.83 (d, J = 6.8 Hz, 6H, CH_3).

In a 100 mL three-neck round-bottom flask, Br−EG_{45}−Br (7.91 g, 3.49×10^{-3} mol) was dissolved in dichloromethane (50 mL) and stirred with pyridine (40 mL). Potassium O-ethyl dithiocarbonate (1.15 g, 7.19×10^{-3} mol) was added portionwise. The mixture was stirred at room temperature for 24 h. The resulting mixture was centrifuged and the white precipitates were removed. Dichloromethane was added (300 mL) to filtrate. The solution was washed with concentrated ammonium chloride (4 × 100 mL), saturated sodium bicarbonate (3 × 100 mL), water (2 × 100 mL), and dried over anhydrous magnesium sulfate. The solvents were evaporated under vacuum. X−EG_{45}−X was obtained (5.85 g, 71.4%). ^{1}H NMR data (400 MHz, $CDCl_3$):δ 4.62 (q, J = 7.2 Hz, 4H, OCH_2CH_3), δ 4.41 (q, J = 7.5 Hz, 2H, $CHCH_3$), δ 4.30 (m, 4H, $CH_2OC(O)$), δ 3.65 (s), δ 3.5−3.8 (m, 183H, CH_2CH_2O of PEG backbone), δ 1.58 (d, J = 7.5 Hz, 6H, $CHCH_3$), δ 1.42 (t, J = 7.2 Hz, 6H, OCH_2CH_3).

Synthesis of Triblock Copolymers X−OVAc-*b*-EG_{45}-*b*-OVAc−X. A typical polymerization was performed as follows. VAc (7.16 g, 8.33×10^{-2} mol), AIBN (0.030 g, 1.83×10^{-4} mol), X−EG_{45}−X (2.10 g, 8.94×10^{-4} mol), THF (9.30 g) were placed into a flask by passing nitrogen gas through the mixture for 1 h in an ice bath. The flask was immersed in an oil bath preheated at 60 °C with stirring for 12 h. The mixture was reprecipitated in cold *n*-hexane for more than twice. The resulting product was dried under vacuum at 40 °C for more than 24 h to get the final product (monomer conversion = 41%, $M_{n\text{-GPC}}$ = 5420 g/mol, PDI = 1.34, $M_{n\text{-NMR}}$ = 4930 g/mol). ^{1}H NMR data (400 MHz, $CDCl_3$): δ 6.55−6.68, δ 4.78−5.08, δ 4.57−4.70, δ 4.05−4.38, δ 3.51−3.84, δ 2.41−2.57, δ 1.94−2.14, δ 1.50−1.94, δ 1.37−1.46, δ 1.13−1.21

Several X−OVAc-*b*-PEG-*b*-OVAc−X triblock copolymers were prepared with different average degrees of polymerization (n) for the VAc block with the same procedure by varying the initial concentration ratios of VAc to X−PEG−X and conversion.

Polymerization of C/W Emulsions. In a typical polymerization,[53] an aqueous solution of monomers (40% w/v in H_2O), $K_2S_2O_8$ initiator (2% w/v based on monomers), surfactant, and PVA were added in a 10 cm^3 stainless steel view autoclave before purging with a slow flow of CO_2 for 5 min to remove any oxygen. The reactor was

then pressurized with liquid CO_2 (20 °C, 110 ± 5 bar), and magnetically stirred (300 rpm) to form a milky white C/W emulsion. The mixing time and speed were kept constant, since it was known that these parameters can affect the size and uniformity of HIPEs.[54] When a stable emulsion had been formed, stirring was further continued at 300 rpm for 60 min before adding a controlled volume of tetramethyl ethylenediamine (TMEDA, 0.1 mL). Stirring was ceased when the temperature started increasing due to the exothermic reaction. The temperature and pressure were kept for 120 min, and then the CO_2 was slowly vented for more than 1 h. The product was recovered as a continuous, white monolithic sample that conformed to the internal dimensions of the reactor. Subsequently, the material was immersed in water to remove excessive initiator and monomers, and then dried by freeze-drying using a Scientz-12N freeze-dryer for more than 24 h.

Characterization. Nuclear magnetic resonance (NMR) spectra were recorded in $CDCl_3$ on a Bruker AV400 MHz spectrometer at room temperature using tetramethylsilane (TMS) as an internal reference. Polymer morphologies were investigated with a FEI Sirion 200 field emission scanning electron microscope (FE-SEM). For SEM analysis, samples were mounted on aluminum studs using adhesive graphite tape and sputter-coated with gold before analysis. Gel permeation chromatography (GPC) was performed with an Agilent 1100 instrument using refractive index detector (RID) and a chromatography column (PLgel 5 μm). THF was used as an eluent at a flow rate of 1.0 mL/min at 30 °C. The calculated molecular weights were based on a calibration curve for polystyrene (PS) standards of narrow polydispersity (Polymer Laboratories). Pore size distributions were recorded by mercury intrusion porosimetry using a Micromeritics Autopore IV 9500 porosimeter. Samples were subjected to a pressure cycle starting at approximately 0.5 psi, increasing to 60000 psi in predefined steps to determine pore size and pore volume. Thermal gravity analysis (TGA) was carried out at a heating rate of 10 °C/min from 30 to 700 °C on a Pyris1 under a nitrogen atmosphere.

Results and Discussion

Preparation of X−PEG−X and Triblock Copolymers X−OVAc-*b*-PEG-*b*-OVAc−X. Here we present the synthesis of various xanthate RAFT agents with different PEG blocks. Initially, the potassium O-ethyl dithiocarbonate was synthesized via the method of Fleet et al.,[55] recrystallized, and then added to a solution of Br−PEG−Br to obtain macro-CTAs (X−PEG−X). The detailed synthesis strategy is described in Scheme 1.

PVAc is a typical example of inexpensive commercial polymer which is also moderately biodegradable, and has recently been investigated in various biomedical applications.[41,43] Although PVAc is one of the most CO_2-philic hydrocarbon polymers discovered so far, the solubility of PVAc is highly dependent on its molecular weight. Previously we reported that PVAc showed high solubility in CO_2 under conditions of practical relevance only when the molecular weight was lower than 3000 g/mol.[34,38] Because the vinyl acetate propagating radical is highly reactive and apt to chain transfer and termination reactions, it is impossible to obtain OVAc with narrow PDI through conventional free-radical polymerization.[38] Living/control radical polymerization of VAc is often problematic, and techniques such as ATRP and NMP are generally not effective. Successful control of VAc polymerization has been reported under a RAFT mechanism mediated by xanthates.[46−48]

In order to obtain X−OVAc-based surfactants with narrow PDI, a series of reactions were conducted. Following an inhibition period, the polymerization proceeded with pseudofirst-order kinetics consistent with a constant radical concentration (Figure 1). The ratio of xanthates concentration to initiator

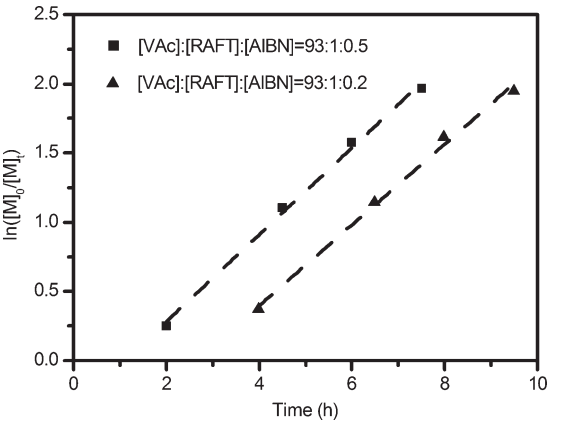

Figure 1. Plots of log of monomer concentration with time for the RAFT polymerization of VAc that mediated by X−EG_{45}−X at 60 °C in a 50% w/w solution in THF. The dashed lines (— —) denote regressed fits to linear relationships.

Scheme 1. Preparation of Macromolecular Chain Transfer Agent X−EG_n−X (n = 13, 45, 77)

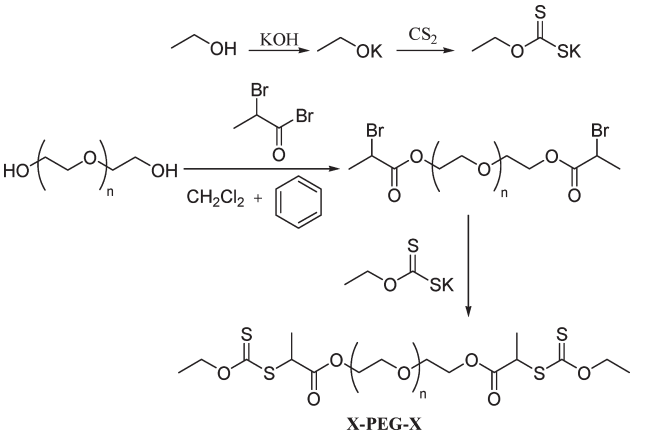

concentration played a crucial role in the inhibition time. When the ratio increased from 2 to 5, the inhibition time intensively raised from 1 to 2.6 h. The evolution of the molecular weight and PDI with conversion during the VAc polymerization in the presence of macroCTA (X−EG_{45}−X) at 60 °C is shown in Figure 2. The GPC chromatograms show a single peak growing with reaction time and conversion (Figure 3). A progressive and nearly linear increase in the molecular weight as a function of conversion is observed, which is consistent with a living process (Figure 2). However, a broad molecular weight distribution of the polymers is observed at high conversion (> 50%) of VAc, which suggests the formation of PVAc homopolymer in the later polymerization stage as reported previously.[51] Interestingly, the homopolymerization is slight at lower conversion. Therefore, we could control the monomer conversion at a relatively low level to prepare OVAc with narrow PDI.

In order to investigate the influence of the molecular weight of OVAc block on the hydrophilic-CO_2-philic balance, a series of copolymers were synthesized by RAFT polymerization mediated by various macroCTAs (Table 1). An advantage of this methodology is that it could directly lead to oligomeric species with relatively low PDI in a range of 1.23−1.35 (Table 1). In all cases, the final products were light yellow viscous liquids because of the incorporation of the xanthate group at the end of the polymers. The xanthate group of X−OVAc-based copolymers could be cleaved from

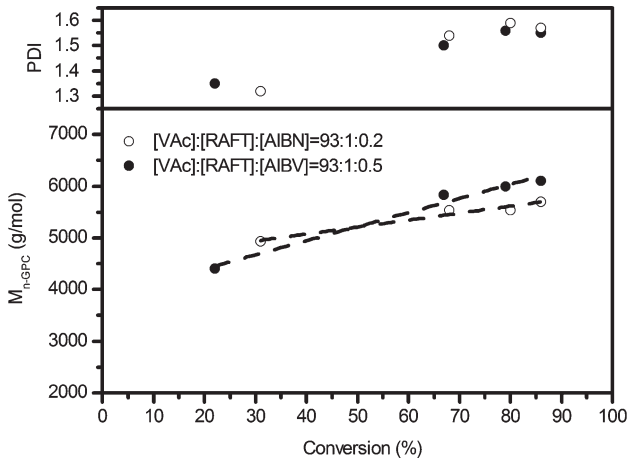

Figure 2. Evolution of the molecular weight and PDI with conversion for the RAFT polymerization of VAc mediated by X−EG_{45}−X at 60 °C in a 50% w/w solution in THF. The dashed lines (— —) denote regressed fits to linear relationships.

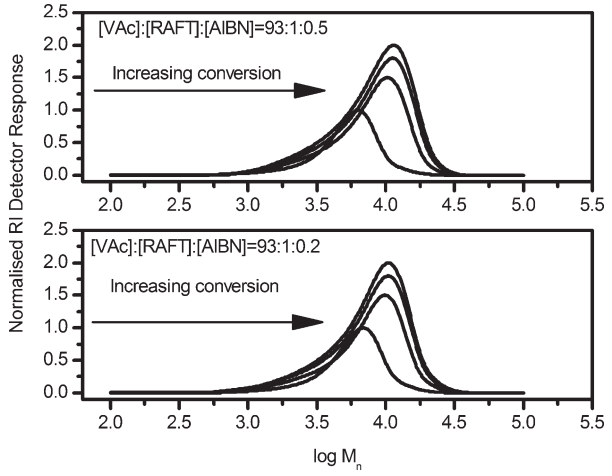

Figure 3. Evolution of GPC traces for the RAFT polymerization of VAc in the presence of X−EG_{45}−X. The reaction was carried out at 60 °C in a 50% w/w solution in THF.

Table 1. Molecular Weight Data of X−OVAc Based Hydrocarbon Surfactants Prepared[a]

polymer composition[b]					
OVAc (g/mol)	PEG (g/mol)	conv[c] (%)	$M_{n\text{-GPC}}$[d] (g/mol)	$M_{n\text{-NMR}}$[e] (g/mol)	PDI[d]
2 × 600	540	18	2270	2100	1.35
2 × 690	2060	14	4420	3730	1.32
2 × 1200	2060	31	5490	4760	1.29
2 × 1290	2060	41	5420	4930	1.34
2 × 1380	2060	46	6060	5100	1.30
2 × 1460	2060	35	6260	5270	1.23
2 × 1810	2060	49	6850	5960	1.23
2 × 510	3340	17	6920	4700	1.27
2 × 980	3340	28	7880	5640	1.29

[a] Reactions were carried out with the molar ratio of [VAc]:[macroCTAs]:[AIBN] is 93:1:0.2 at 60 °C in a 50% w/w solution in THF. [b] Calculated from $M_{n\text{-NMR}}$. [c] Monomer conversion that determined gravimetrically after evaporation of the solvent and monomer. [d] Determined by GPC. [e] Determined via ^{1}H NMR spectroscopy analysis of the polymers.

polymers by thermolysis as reported previously.[56] Thermogravimetric analysis of X−OVAc-*b*-EG_{45}-*b*-OVAc−X ($M_{n\text{-NMR}}$ = 4930 g/mol, PDI = 1.34) showed a mass loss of 6.8% between 210 and 310 °C, which was consistent with the loss of the xanthate group (7.1%, expected for $C_3H_5S_2$) (Figure 4).

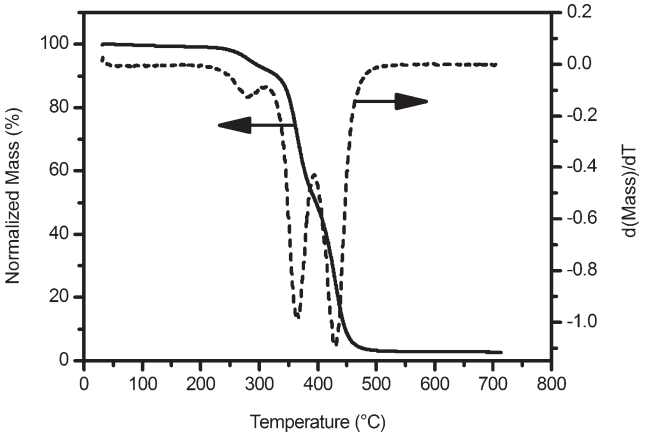

Figure 4. Normalized mass loss (—) and first derivative of mass loss (- - -) for X−OVAc-*b*-PEG-*b*-OVAc−X ($M_{n\text{-NMR}}$ = 4930 g/mol, PDI = 1.31) heated from 30 to 700 at 10 °C/min under nitrogen.

The structures of the starting macroCTAs and its corresponding copolymers were characterized by ^{1}H NMR to confirm the incorporation of VAc units into the macroCTAs (Supporting Information, Figures S9 and S10).[51] The number-average molecular weights of those copolymers calculated by ^{1}H NMR from the relative integrations of $-CH_2-CH_2-O-$ protons of PEG backbone and of the $-CH-$ protons of VAc backbone are also listed (Table 1). The experimental molecular weights evaluated from GPC show a slight deviation from that calculated from ^{1}H NMR. The main reason may be the difference in the hydrodynamic volumes of PEG and PS (which was used as the calibration standard) to a certain extent.

Formation of Stable C/W Emulsions. It is well-known that low molecular weight perfluoropolyether (PFPE) ammonium carboxylate surfactants can be employed to form both C/W and W/C macroemulsions[57] and microemulsions.[21,58,59] However, the C/W macroemulsions stabilized by PFPE are not much stable in the presence of monomers, such as AM and MBAM.[60] There can be two reasonable possibilities for this phenomenon. First, the monomers adsorb at the water−CO_2 interface, thus reducing interfacial tension gradients and, therefore, stability of the emulsions.[57] Another possibility could be that the monomers play a crucial role in the solution properties of the surfactant in the aqueous phase, that is, the surfactant becomes more soluble in the aqueous phase and, hence, is removed from the C/W interface.[53] Although this destabilization can be overcome by the addition of cosurfactant (PVA) to the aqueous phase prior to polymerization, perfluorinated surfactants are much more expensive and insufficiently degradable for many applications.

Johnston has reported that less expensive hydrocarbon surfactants such as poly(ethylene oxide)-*b*-poly(butylene oxide) (EO_{15}-*b*-BO_{12}) could be used to emulsify up to 70% CO_2 with droplet sizes from 2 to 4 μm in diameter, as determined by video-enhanced microscopy.[61] In our previous study,[37] we synthesized various OVAc-based hydrocarbon surfactants, which could stabilize highly concentrated C/W emulsions. However, the practical industrial applications of such surfactants were limited due to various factors as described above. In order to address these issues, we have prepared a series of X−OVAc-based hydrocarbon surfactants to investigate the emulsification of CO_2 and an aqueous solution (40% w/v AM + MBAM in H_2O, AM/MBAM = 8:2 w/w), as detailed in Table 2. Interestingly, even without addition of cosurfactant (PVA), these emulsions were found to be stable for a long period in the absence of stirring (i.e., more than 24 h).

Table 2. Stability of C/W Emulsion Prepared Using X−OVAc-based surfactants

	X−OVAc-*b*-PEG-*b*-OVAc−X				
	OVAc[a] (g/mol)	PEG (g/mol)	% (w/v)	C/W[b] (v/v)	note
1	2 × 600	540	1	8:2	partial emulsion, 100−250 bar
2	2 × 1370	540	1	8:2	partial emulsion, 100−250 bar
3	2 × 690	2060	1	9:1	stable emulsion at 65 bar, 24 h
4	2 × 1290	2060	0.16	8:2	stable emulsion at 110 bar, 3 h
5	2 × 1290	2060	1	9:1	stable emulsion at 110 bar, 24 h
6	2 × 1810	2060	1	8:2	stable emulsion at 110 bar, 6 h
7	2 × 1810	2060	1	9:1	stable emulsion at 110 bar, 24 h
8[c]	3600	2000	1	8:2	partial emulsion, 100−300 bar
9	2 × 510	3340	1	9:1	partial emulsion, 100−250 bar
10	2 × 980	3340	1	9:1	stable emulsion at 100 bar, 24 h

[a] Calculated from the equation of $(M_{n\text{-NMR}} - M_{PEG})/2$. [b] An aqueous solution of AM + MBAM (40% w/v in H_2O, AM/MBAM = 8:2 w/w) without PVA. [c] Taken from ref 38.

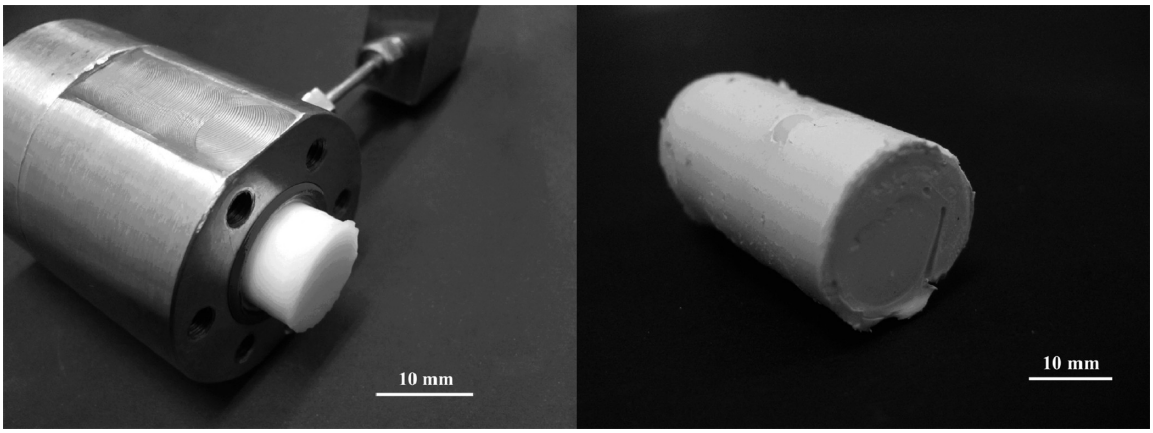

Figure 5. Photograph of a low-density C/W emulsion templated PAM-based materials. The materials obtained conform closely to the cylindrical interior of the reaction vessel.

Table 3. Synthesis of C/W Emulsion-Templated PAM materials Using Hydrocarbon Surfactants [a]

	X−OVAc-*b*-PEG-*b*-OVAc−X						
PAM	OVAc (g/mol)	PEG (g/mol)	% (w/v)	PVA (w/v)	CO_2/H_2O (v/v)	median pore diameter (μm)[b]	total intrusion volume (cm^3/g)[b]
1	2 × 1290	2060	2	1	8:2	5.22	6.65
2	2 × 1290	2060	1	1	8:2	5.04	5.30
3	2 × 1290	2060	0.5	1	8:2	6.83	6.21
4	2 × 1290	2060	0.25	1	8:2	10.29	7.82
5	2 × 1290	2060	1	0	8:2	5.45	7.47
6	2 × 1290	2060	0.25	0	8:2	7.47	4.66
7	2 × 1290	2060	0.5	0	9:1	8.10	7.71
8	2 × 690	2060	1	0	8:2	7.19	7.42
9	2 × 1810	2060	1	0	8:2	5.12	6.58
10[c]	2 × 2110	2000	1	10	8:2	5.55	7.51

[a] Reaction conditions: AM + MBAM (40% w/v in H_2O, AM/MBAM = 8:2 w/w), $K_2S_2O_8$ (2% w/v based on monomer), surfactant, PVA (M_w = 74800 g/mol, 99% hydrolyzed), 20 °C, 110 bar, 2 h, venting, and then freeze-drying. [b] Measured by mercury intrusion porosimetry over the range 7 nm to 100 μm. [c] Taken from ref 38.

Neither PEG, OVAc, nor a mixture of these two materials could form stable C/W emulsions.[38] This demonstrated the requirement for the amphiphilic block copolymer structure. However, not all X−OVAc-based hydrocarbon surfactants can lead to stable emulsions. It was found that surfactants with a short PEG block ($M_{n\text{-NMR}}$ = 540 g/mol) were poor stabilizers for C/W emulsions (Table 2, samples 1, 2). However, when the molecular weight of PEG block increased to 2060 g/mol, it was observed that highly concentrated milky-white C/W emulsions were formed, which filled the entire reaction vessel. Neither too high molecular weight of OVAc block, nor too low molecular weight could lead to such stable emulsions (Table 2, samples 8, 9). These results agree well with the fact that achieving an appropriate hydrophilic-CO_2-philic balance for surfactants is a key factor for C/W emulsion stability. It is considerably easy to adjust this balance through the control of molecular weights of OVAc block and PEG block via RAFT polymerization.

The emulsions showed remarkable stability against coalescence for several hours in the absence of stirring. It was noteworthy that with the internal phase volume increasing from 80% to 90%, the stability of emulsion was dramatically enhanced. In previous reports,[62] it has been demonstrated that increasing the internal phase volume caused the viscosity of the system to increase. Therefore, the main possible reason for this larger increase in emulsion stability may be that the increase of internal phase volume causes an increase in the interfacial viscosity, thus inhibiting the tangential interfacial flow in the thin aqueous film between the CO_2 droplets.

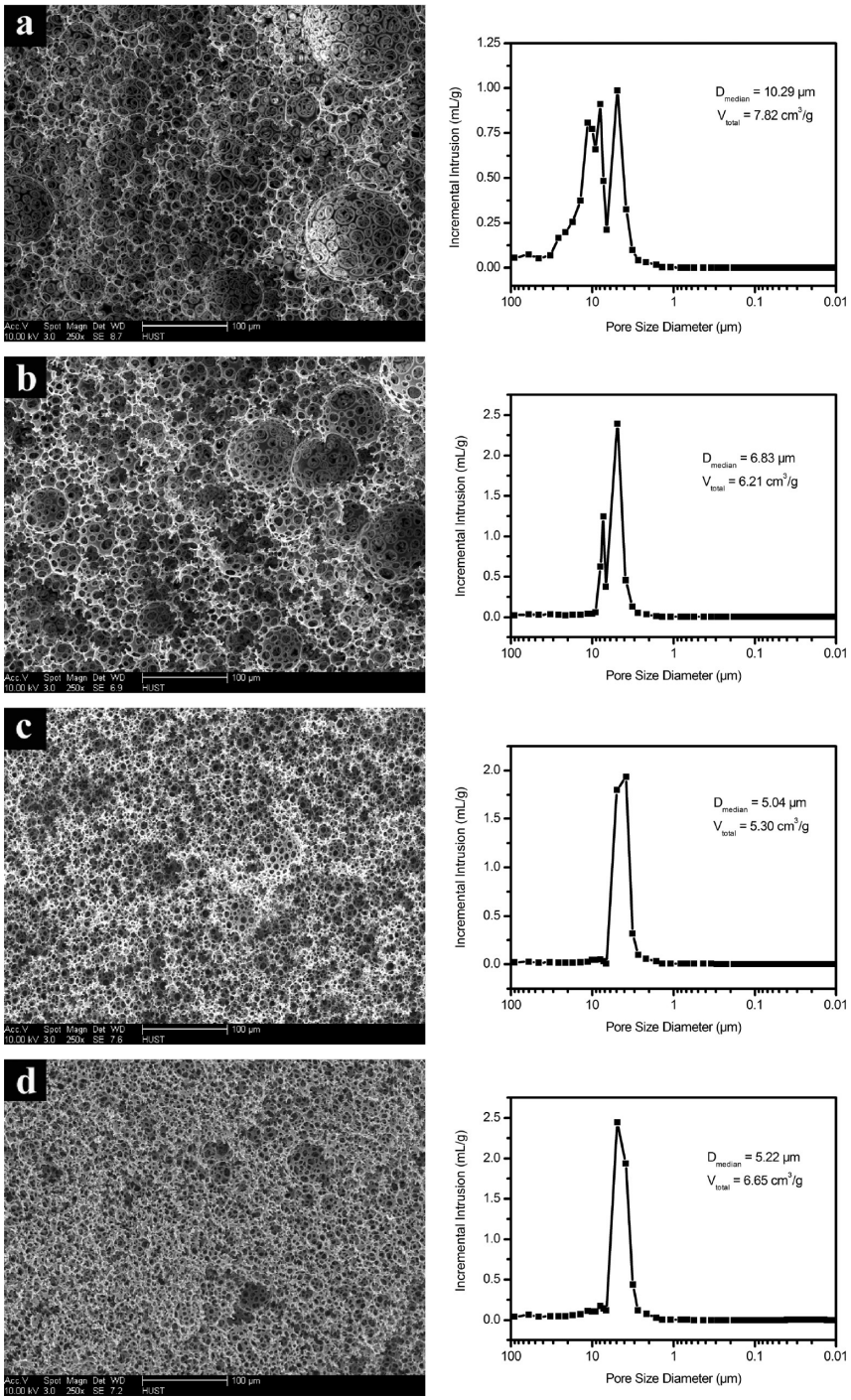

Figure 6. Porous PAM-based materials prepared by C/W emulsion templating with different surfactant concentrations (X−OVAc(1290)-*b*-PEG-(2060)-*b*-OVAc(1290)−X), as characterized by scanning electron microscopy (left) and mercury intrusion porosimetry (right). The experimental details listed in the Table 3. Key: (a) sample 4, 0.25% w/v; (b) sample 3, 0.5% w/v; (c) sample 2, 1.0% w/v; (d) sample 1, 2.0% w/v.

In our previous study, it was reported that the emulsions, stabilized by PFPE, would undergo phase separation by the addition of monomers (AM and MBAM) without cosurfactant (PVA). In contrast, the X−OVAc-based surfactants could stabilize highly concentrated C/W emulsions (90% CO_2) in the presence of such monomers without PVA (Table 2). Interestingly, surfactant at concentration as low as 0.16 wt % is sufficient to form a relative stable highly concentrated C/W emulsions and effectively inhibit CO_2 droplets from further coalescence (Table 2, sample 4). This finding is in contrast to conventional HIPEs,[1,53] for which large fractions of expensive surfactants (2−50%) are often required to stabilize HIPEs effectively.

In summary, these results suggest that X−OVAc-based surfactants are very effective in the formation of stable and highly concentrated C/W emulsions. Therefore, the emulsion templating approach to produce porous materials is feasible, because the free-radical polymerization would be expected to occur before the emulsion became destabilized.

PAM-Based Materials. Although successful C/W emulsion-templated polymerization has been carried out, the systems provided so far have involved fluorinated surfactants (PFPE) which are very expensive and are not environmental friendly.[22,53,60] Many conventional hydrocarbon surfactants used in O/W systems exhibit low solubility in CO_2

and are incapable of generating either W/C or C/W emulsions.[63] Despite the fact that several commercial hydrocarbon surfactants (e.g., sodium dodecylbenzenesulfonate (SDBS), Tween 40) were exploited as stabilizers to prepare porous emulsion-templated materials, none of these hydrocarbon surfactants, however, gave rise to pore volumes as high as those obtained for samples using PFPE surfactants. The resultant materials were less porous and less well-defined than when PFPE was used and the concentration of surfactants was also as high as 10% which raised the cost of related applications.[53]

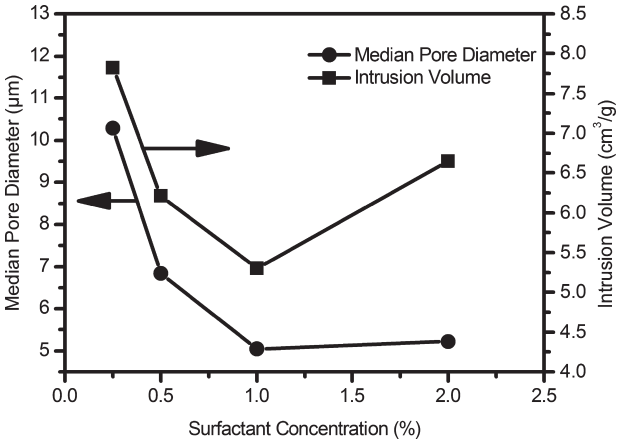

Figure 7. Effect of surfactant concentrations (Table 3, samples 1−4) on the intrusion volume, median pore diameter of C/W emulsion-templated porous PAM-based materials.

In this study, we reported a versatile method to directly synthesize various X−OVAc-based surfactants used to stabilize C/W HIPEs. In the presence of these X−OVAc-based surfactants, it was observed that the C/W HIPEs were sufficiently stable to act as templates for the formation of polyHIPEs. A catalytic amount of a redox co-initiator (TMEDA)[53] was used to initiate these polymerization reactions at 20 °C. The remarkable stability of the C/W emulsions was further demonstrated by polymerization of the continuous aqueous phase to produce porous, cross-linked PAM-based materials. The emulsion-templated materials were recovered as uniform monoliths with a smooth surface, which conformed closely to the cylindrical interior of the reactor (Figure 5), suggesting that most of the CO_2 was emulsified and templated. The resulted emulsion-templated materials were soaked in

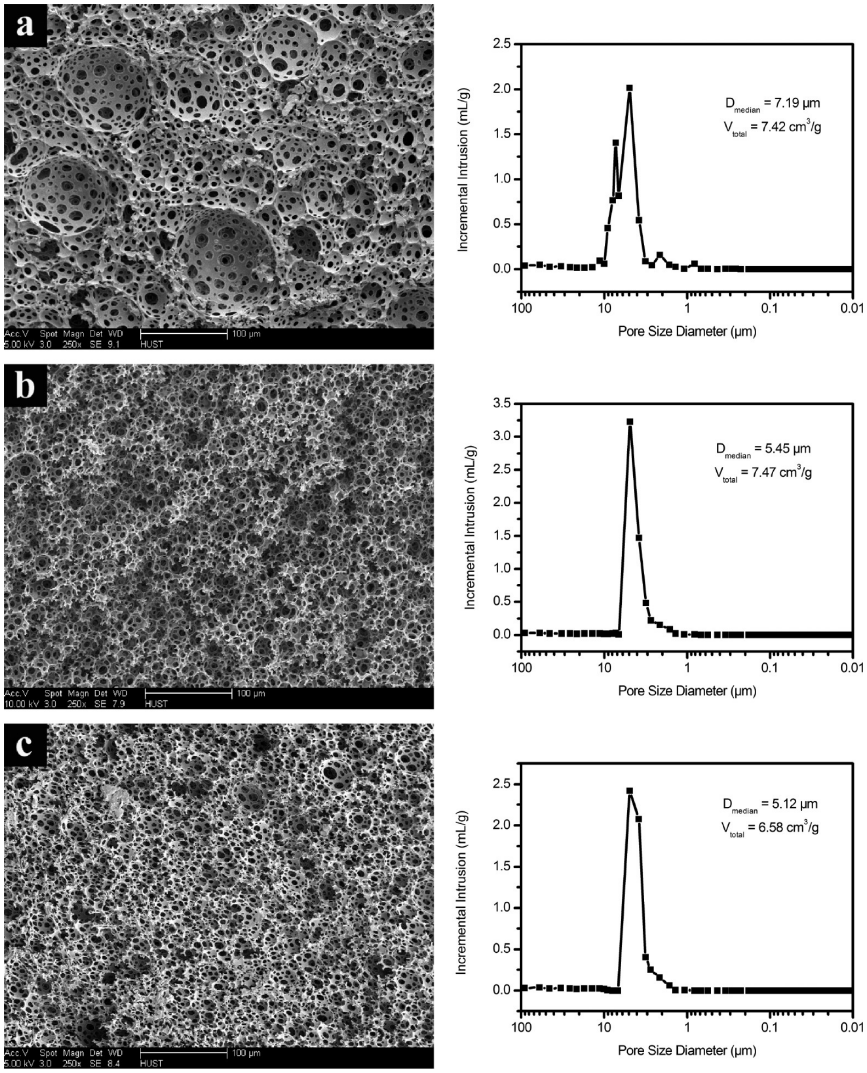

Figure 8. PAM-based porous materials synthesized by C/W emulsion templating with various molecular weight of X−OVAc-based surfactants as characterized by scanning electron microscopy (left) and mercury intrusion porosimetry (right). The experimental details are listed in the Table 3. (a) Sample 8, X−OVAc(690)-*b*-PEG(2060)-*b*-OVAc(690)−X. (b) Sample 5, X−OVAc(1290)-*b*-PEG(2060)-*b*-OVAc(1290)−X. (c) Sample 9, X−OVAc(1810)-*b*-PEG(2060)-*b*-OVAc(1810)−X.

water to remove residual initiator and monomers, and then freeze-dried. When the dried samples were placed in water, their shapes were recovered completely within a few seconds. The pore characterization data of the C/W emulsion-templated materials are summarized in Table 3. The SEM images (Figure 6, 8) of the monoliths indicated that the open-cell porous morphology was obtained.

A comparison of the pore properties of emulsion-templated materials using OVAc-based and X−OVAc-based hydrocarbon surfactants is provided (Table 3, samples 9 and 10). The results show that the RAFT terminus has only a small influence upon the pore properties of the materials. The highest pore volume (7.81 cm^3/g) is observed in sample 4 produced by using 0.25% w/v X−OVAc(1290)-*b*-PEG-(2060)-*b*-OVAc(1290)−X, which is much more porous than produced by using PFPE surfactant (5.89 cm^3/g).[53] This result suggests that X−OVAc-based hydrocarbon surfactants are superior to perfluorinated surfactants and approach OVAc-based hydrocarbon surfactants for this application. To tailor the morphology of the porous structures, the influence of the surfactant concentration and OVAc block molecular weight are also investigated.

Effect of X−OVAc-Based Surfactant Concentration. A series of C/W emulsion-templated porous materials were synthesized over a range of surfactant concentration (0.25−2% w/v). All the variables, such as mixing time, mixing speeds, monomer concentration, initiator concentration, CO_2 volume, and CO_2 pressure, were kept constant. Figure 6 shows a series of SEM images and mercury intrusion porosimetry plots for the emulsion-templated materials synthesized at increasing surfactant concentration. It should be noted that the discontinuity that can be observed at around 7.5 μm in many of the porosimetry plots (e.g., Figure 6a) is an artifact that arises from switching the analysis from the low-pressure port (large pores) to the high-pressure port (small pores). The median pore diameter (5.04−10.29 μm) is measured by mercury intrusion porosimetry and corresponds to the average size of interconnected pore that connect the emulsion-templated CO_2 droplets. The cell diameter can be observed from SEM images and has, approximately, the same average diameter as that of CO_2 emulsion droplets immediately prior to chemical gelation of the system. The effect of surfactant concentration on the intrusion volume and median pore diameter is also shown in Figure 7. The intrusion volume in these materials shows a minimum of 5.30 cm^3/g at a surfactant concentration of around 1.0% w/v. Interestingly, decreasing the amount of surfactant from 2 to 0.25 wt % dramatically increases the size of interconnected pores and cells, which is in accordance with dominant micellar nucleation mechanism proposed by Harkins.[64] According to the mechanism, an increase in the ratio of initial surfactant to monomer increases the relative amount of micelles and should increase the number of the CO_2 droplets, thus decreasing the size of the CO_2 droplets. After polymerization, venting, the size of cells also decreases correspondingly. These predictions are in accordance with the experimental results (Figure 6).

In previous study, we found that C/W emulsion droplets were much more heterogeneous, as evident from the distribution of cell sizes observed in the scanning electron micrographs.[53] The materials shown in Figure 6c,d are significantly more homogeneous, while the SEM images for the samples with a low surfactant concentration (typically less than 0.5% w/v) indicate broad cell distribution (Figure 6a,b). The possible reason for such broad cell distribution could be that the addition of small amount of surfactant leads to destabilization by bridging flocculation between droplets,[65] where a single polymer molecule may adsorb two or more CO_2 droplets, physically hold them together, and result in coalescence to some extent, that is, large cells are surrounded by much smaller cells. The experimental results strongly support that the morphology of the monoliths of Figure 6a is due to bridging flocculation. Sample 6 (Table 3) shows the lowest intrusion volume (4.66 cm^3/g). In this experiment, the surfactant concentration is as low as 0.25% w/v in the absence of cosurfactant (PVA), which would lead to partial droplet coalescence.

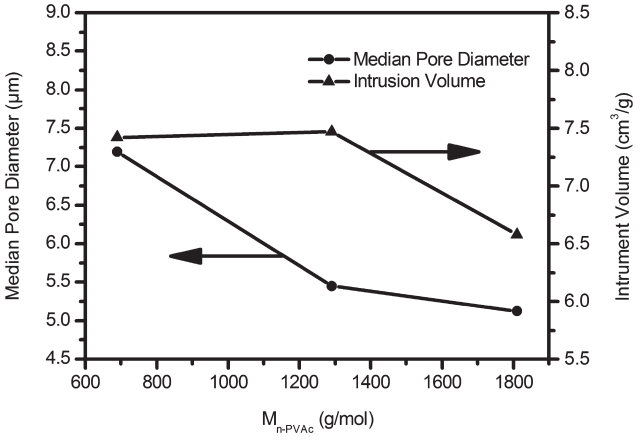

Figure 9. Effect of molecular weight of OVAc block (Table 3, samples 5, 8, 9) on the intrusion volume, median pore diameter of C/W emulsion-templated porous PAM-based materials.

An attractive feature of the approach described above is that the size of the final structure can be tunable by simply changing the surfactant concentration. Under such circumstances, it is possible to obtain porous materials with cell diameter of 100 μm required as a scaffold for tissue engineering applications.

Effect of OVAc Block Molecular Weight. In our previous study, we have demonstrated that the solubility of the OVAc in CO_2 strongly depended on the molecular weight, with the concept that the OVAc molecular weight could affect the hydrophilic-CO_2-philic balance of the C/W emulsions, and thus affect the pore properties of the C/W emulsion-templated materials. A series of PAM-based emulsion-templated materials were synthesized at a constant surfactant concentration (1% w/v based on reactor) over a range of OVAc block molecular weights ($M_{n\text{-}NMR}$ = 690−1810 g/mol, Table 3, samples 5, 8 and 9). It is obvious that the interconnected pore diameter in those materials decreases with increasing the OVAc block molecular weight (Figure 9), which suggests that the hydrophilic-CO_2-philic balance plays an important role in the formation of these emulsions. This tendency can also be observed in SEM images (Figure 8). The intrusion volume shows a maximum of approximately 7.47 cm^3/g at the OVAc block molecular weight of around 1290 g/mol. Compared with the samples 5, 8, and 9, the intrusion volumes for samples 5 and 8 (Table 3) are similar (7.42 vs 7.47 cm^3/g), however, it decreases rapidly for sample 9 (6.58 cm^3/g). This result is consistent with the solubility decreasing with increasing OVAc block molecular weight, which would affect the stability of emulsions, and then result in partial CO_2 droplets coalescence, but does not proceed to the formation of two separate phases.

Conclusions

In summary, we present here a versatile method for preparation of X−OVAc-based hydrocarbon surfactants with narrow PDI (< 1.35) for the production of C/W emulsions. Xanthate end-functional PEGs acting as macroCTAs were exploited to mediate the polymerization of VAc. Compared with the synthesis

of OVAc-based surfactants, the process of the preparation of X−OVAc-based surfactants was much more simple, inexpensive and also easy to control, which could promote industrial-scale applications. It was shown that X−OVAc-based surfactants can effectively stabilize highly concentrated C/W emulsions. Highly porous emulsion-templated materials with tunable cells size and interconnected pores size were also prepared by the polymerization of the continuous phase of C/W emulsions. The influence of the surfactant concentration and molecular weight of OVAc block on the morphology of the porous structures were also investigated. The analysis by mercury intrusion porosimetry confirms the interconnected pore size in the range of 3.2−10.0 μm and the intrusion volume in the range of 4.66−7.82 cm^3/g. These results indicate that X−OVAc-based surfactants can outperform perfluorinated analogues and approach the OVAc-based surfactants for this application. X−OVAc-based surfactants may develop a range of potential applications in emulsion technology such as the generation of biodegradable scaffolds with highly interconnected pores suitable for tissue engineering scaffolds.

Acknowledgment. The authors thank Irshad Hussain of the National Institute for Biotechnology and Genetic Engineering for fruitful discussions. We also thank National Natural Science Foundation of China (No. 20774032) for financial support, and the Analytical and Testing Center of Huazhong University of Science & Technology for characterization assistance. B.T. gratefully acknowledges the award of a Program for New Century Excellent Talents in University (NCET-10-0389).

Supporting Information Available: Figures showing C/W emulsion-templated polymerization equipment, kinetics data and GPC data, ^{1}H NMR data of Br−EG_n−Br, X−EG_n−X (n = 13, 45), and their copolymers, SEM images, median pore size distributions, and the C/W emulsions, respectively. This material is available free of charge via the Internet at http://pubs.acs.org.

References and Notes

(1) Cameron, N. R. *Polymer* **2005**, *46*, 1439–1449.
(2) Christenson, E. M.; Soofi, W.; Holm, J. L.; Cameron, N. R.; Mikos, A. G. *Biomacromolecules* **2007**, *8*, 3806–3814.
(3) Qian, L.; Ahmed, A.; Foster, A.; Rannard, S. P.; Cooper, A. I.; Zhang, H. F. *J. Mater. Chem.* **2009**, *19*, 5212–5219.
(4) Imhof, A.; Pine, D. J. *Nature* **1997**, *389*, 948–951.
(5) Kuschel, A.; Polarz, S. *J. Am. Chem. Soc.* **2010**, *132*, 6558–6565.
(6) Galarneau, A.; Calin, N.; Iapichella, J.; Barrande, M.; Denoyel, R.; Coasne, B.; Fajula, F. *Chem. Mater.* **2009**, *21*, 1884–1892.
(7) Wang, Y.; Caruso, F. *Chem. Mater.* **2006**, *18*, 4089–4100.
(8) DeSimone, J. M. *Science* **2002**, *297*, 799–803.
(9) Cooper, A. I. *Adv. Mater.* **2001**, *13*, 1111–1114.
(10) Cooper, A. I. *J. Mater. Chem.* **2000**, *10*, 207–234.
(11) Beckman, E. J. *Chem. Commun.* **2004**, 1885–1888.
(12) Chen, K. P.; Liang, L. Y.; Tan, B. *Prog. Chem.* **2009**, *21*, 2199–2204.
(13) Cooper, A. I.; Wood, C. D.; Holmes, A. B. *Ind. Eng. Chem. Res.* **2000**, *39*, 4741–4744.
(14) Desimone, J. M.; Maury, E. E.; Menceloglu, Y. Z.; McClain, J. B.; Romack, T. J.; Combes, J. R. *Science* **1994**, *265*, 356–359.
(15) DeSimone, J. M.; Guan, Z.; Elsbernd, C. S. *Science* **1992**, *257*, 945–947.
(16) Fink, R.; Hancu, D.; Valentine, R.; Beckman, E. J. *J. Phys. Chem. B* **1999**, *103*, 6441–6444.
(17) Cooper, A. I.; Londono, J. D.; Wignall, G.; McClain, J. B.; Samulski, E. T.; Lin, J. S.; Dobrynin, A.; Rubinstein, M.; Burke, A. L. C.; Frechet, J. M. J.; DeSimone, J. M. *Nature* **1997**, *389*, 368–371.
(18) Thurecht, K. J.; Gregory, A. M.; Wang, W.; Howdle, S. M. *Macromolecules* **2007**, *40*, 2965–2967.
(19) Gregory, A. M.; Thurecht, K. J.; Howdle, S. M. *Macromolecules* **2008**, *41*, 1215–1222.
(20) Zong, M. M.; Thurecht, K. J.; Howdle, S. M. *Chem. Commun.* **2008**, 5942–5944.
(21) Johnston, K. P.; Harrison, K. L.; Clarke, M. J.; Howdle, S. M.; Heitz, M, P.; Bright, F. V.; Carlier, C.; Randolph, T. W. *Science* **1996**, *271*, 624–626.
(22) Palocci, C.; Barbetta, A.; La Grotta, A.; Dentini, M. *Langmuir* **2007**, *23*, 8243–8251.
(23) Beckman, E. J. *J. Supercrit. Fluids* **2004**, *28*, 121–191.
(24) Tan, B.; Woods, H. M.; Licence, P.; Howdle, S. M.; Cooper, A. I. *Macromolecules* **2005**, *38*, 1691–1698.
(25) Sarbu, T.; Styranec, T. J.; Beckman, E. J. *Ind. Eng. Chem. Res.* **2000**, *39*, 4678–4683.
(26) Raveendran, P.; Wallen, S. L. *J. Am. Chem. Soc.* **2002**, *124*, 7274–7275.
(27) Raveendran, P.; Wallen, S. L. *J. Am. Chem. Soc.* **2002**, *124*, 12590–12599.
(28) Fan, X.; Potluri, V. K.; McLeod, M. C.; Wang, Y.; Liu, J. C.; Enick, R. M.; Hamilton, A. D.; Roberts, C. B.; Johnson, J. K.; Beckman, E. J. *J. Am. Chem. Soc.* **2005**, *127*, 11754–11762.
(29) Hong, L.; Tapriyal, D.; Enick, R. M. *J. Chem. Eng. Data* **2008**, *53*, 1342–1345.
(30) Wang, Y.; Hong, L.; Tapriyal, D.; Kim, I. C.; Paik, I. H.; Crosthwaite, J. M.; Hamilton, A. D.; Thies, M. C.; Beckman, E. J.; Enick, R. M.; Johnson, J. K. *J. Phys. Chem. B* **2009**, *113*, 14971–14980.
(31) Lee, H.; Pack, J. W.; Wang, W.; Thurecht, K. J.; Howdle, S. M. *Macromolecules* **2010**, *43*, 2276–2282.
(32) Lee, H.; Terry, E.; Zong, M.; Arrowsmith, N.; Perrier, S.; Thurecht, K. J.; Howdle, S. M. *J. Am. Chem. Soc.* **2008**, *130*, 12242–12243.
(33) Kilic, S.; Wang, Y.; Johnson, J. K.; Beckman, E. J.; Enick, R. M. *Polymer* **2009**, *50*, 2436–2444.
(34) Tan, B.; Bray, C. L.; Cooper, A. I. *Macromolecules* **2009**, *42*, 7945–7952.
(35) Kilic, S.; Michalik, S.; Wang, Y.; Johnson, J. K.; Enick, R. M.; Beckman, E. J. *Macromolecules* **2007**, *40*, 1332–1341.
(36) Shen, Z.; McHugh, M. A.; Xu, J.; Belardi, J.; Kilic, S.; Mesiano, A.; Bane, S.; Karnikas, C.; Beckman, E.; Enick, R. *Polymer* **2003**, *44*, 1491–1498.
(37) Tan, B.; Cooper, A. I. *J. Am. Chem. Soc.* **2005**, *127*, 8938–8939.
(38) Tan, B.; Lee, J.-Y.; Cooper, A. I. *Macromolecules* **2007**, *40*, 1945–1954.
(39) Lee, J.-Y.; Tan, B.; Cooper, A. I. *Macromolecules* **2007**, *40*, 1955–1961.
(40) Lipscomb, C. E.; Mahanthappa, M. K. *Macromolecules* **2009**, *42*, 4571–4579.
(41) Bernard, J.; Favier, A.; Davis, T. P.; Barner-Kowollik, C.; Stenzel, M. H. *Polymer* **2006**, *47*, 1073–1080.
(42) Bernard, J.; Favier, A.; Zhang, L.; Nilasaroya, A.; Davis, T. P.; Barner-Kowollik, C.; Stenzel, M. H. *Macromolecules* **2005**, *38*, 5475–5484.
(43) Stenzel, M. H.; Davis, T. P.; Barner-Kowollik, C. *Chem. Commun.* **2004**, 1546–1547.
(44) Gray, M. K.; Zhou, H. Y.; Nguyen, S. T.; Torkelson, J. M. *Macromolecules* **2004**, *37*, 5586–5595.
(45) Bergenudd, H.; Coullerez, G.; Jonsson, M.; Malmstrom, E. *Macromolecules* **2009**, *42*, 3302–3308.
(46) Barner-Kowollik, C.; Perrier, S. *J. Polym. Sci., Part A: Polym. Chem.* **2008**, *46*, 5715–5723.
(47) Destarac, M.; Charmot, D.; Franck, X.; Zard, S. Z. *Macromol. Rapid Commun.* **2000**, *21*, 1035–1039.
(48) Stenzel, M. H.; Cummins, L.; Roberts, G. E.; Davis, T. P.; Vana, P.; Barner-Kowollik, C. *Macromol. Chem. Phys.* **2003**, *204*, 1160–1168.
(49) Debuigne, A.; Caille, J. R.; Jerome, R. *Angew. Chem., Int. Ed.* **2005**, *44*, 1101–1104.
(50) Peng, C.-H.; Scricco, J.; Li, S.; Fryd, M.; Wayland, B. B. *Macromolecules* **2008**, *41*, 2368–2373.
(51) Pound, G.; Aguesse, F.; McLeary, J. B.; Lange, R. F. M.; Klumperman, B. *Macromolecules* **2007**, *40*, 8861–8871.
(52) Tong, Y. Y.; Dong, Y. Q.; Du, F. S.; Li, Z. C. *J. Polym. Sci., Part A: Polym. Chem.* **2009**, *47*, 1901–1910.
(53) Butler, R.; Hopkinson, I.; Cooper, A. I. *J. Am. Chem. Soc.* **2003**, *125*, 14473–14481.
(54) Cameron, N. R.; Sherrington, D. C. *Adv. Polym. Sci.* **1996**, *126*, 163–214.
(55) Fleet, R.; McLeary, J. B.; Grumel, V.; Weber, W. G.; Matahwa, H.; Sanderson, R. D. *Macromol. Symp.* **2007**, *255*, 8–19.

(56) Postma, A.; Davis, T. P.; Evans, R. A.; Li, G. X.; Moad, G.; O'Shea, M. S. *Macromolecules* **2006**, *39*, 5293–5306.
(57) Lee, C. T.; Psathas, P. A.; Johnston, K. P.; deGrazia, J.; Randolph, T. W. *Langmuir* **1999**, *15*, 6781–6791.
(58) Lee, C. T.; Ryoo, W.; Smith, P. G.; Arellano, J.; Mitchell, D. R.; Lagow, R. J.; Webber, S. E.; Johnston, K. P. *J. Am. Chem. Soc.* **2003**, *125*, 3181–3189.
(59) Heitz, M. P.; Carlier, C.; deGrazia, J.; Harrison, K. L.; Johnston, K. P.; Randolph, T. W.; Bright, F. V. *J. Phys. Chem. B* **1997**, *101*, 6707–6714.
(60) Butler, R.; Davies, C. M.; Cooper, A. I. *Adv. Mater.* **2001**, *13*, 1459–1463.
(61) da Rocha, S. R. P.; Psathas, P. A.; Klein, E.; Johnston, K. P. *J. Colloid Interface Sci.* **2001**, *239*, 241–253.
(62) Barbetta, A.; Cameron, N. R.; Cooper, S. J. *Chem. Commun.* **2000**, 221–222.
(63) Consan, K. A.; Smith, R. D. *J. Supercrit. Fluids* **1990**, *3*, 51–65.
(64) Harkins, W. D. *J. Am. Chem. Soc.* **1947**, *69*, 1428–1444.
(65) Dickinson, E.; Golding, M.; Povey, M. J. W. *J. Colloid Interface Sci.* **1997**, *185*, 515–529.